The ISME Journal (2015) 9, 1306–1318

www.nature.com/ismej

OPEN

ORIGINAL ARTICLE

Spatial scales of bacterial community diversity at cold seeps (Eastern Mediterranean Sea)

Petra Pop Ristova[1,2,3], Frank Wenzhöfer[1,2,3], Alban Ramette[1,2], Janine Felden[1,2,3] and Antje Boetius[1,2,3]

[1]*HGF-MPG Group for Deep Sea Ecology and Technology, Alfred-Wegener-Institut Helmholtz Zentrum für Polar und Meeresforschung, Bremerhaven, Germany;* [2]*Max Planck Institute for Marine Microbiology, Bremen, Germany and* [3]*MARUM—Centre for Marine Environmental Science, University of Bremen, Bremen, Germany*

Cold seeps are highly productive, fragmented marine ecosystems that form at the seafloor around hydrocarbon emission pathways. The products of microbial utilization of methane and other hydrocarbons fuel rich chemosynthetic communities at these sites, with much higher respiration rates compared with the surrounding deep-sea floor. Yet little is known as to the richness, composition and spatial scaling of bacterial communities of cold seeps compared with non-seep communities. Here we assessed the bacterial diversity across nine different cold seeps in the Eastern Mediterranean deep-sea and surrounding seafloor areas. Community similarity analyses were carried out based on automated ribosomal intergenic spacer analysis (ARISA) fingerprinting and high-throughput 454 tag sequencing and were combined with *in situ* and *ex situ* geochemical analyses across spatial scales of a few tens of meters to hundreds of kilometers. Seep communities were dominated by *Deltaproteobacteria*, *Epsilonproteobacteria* and *Gammaproteobacteria* and shared, on average, 36% of bacterial types (ARISA OTUs (operational taxonomic units)) with communities from nearby non-seep deep-sea sediments. Bacterial communities of seeps were significantly different from those of non-seep sediments. Within cold seep regions on spatial scales of only tens to hundreds of meters, the bacterial communities differed considerably, sharing <50% of types at the ARISA OTU level. Their variations reflected differences in porewater sulfide concentrations from anaerobic degradation of hydrocarbons. This study shows that cold seep ecosystems contribute substantially to the microbial diversity of the deep-sea.
The ISME Journal (2015) **9,** 1306–1318; doi:10.1038/ismej.2014.217; published online 12 December 2014

Introduction

Cold seeps are seafloor ecosystems fueled by chemical energy originating from microbial transformation of hydrocarbons and sulfide. They are characterized by the largest biomass and highest productivity of all deep-sea ecosystems (Jørgensen and Boetius, 2007; Levin and Sibuet 2012; Boetius and Wenzhöfer 2013). Because of the localized, spatially and temporarily dynamic supply of hydrocarbons from deep subsurface reservoirs, cold seeps have a highly fragmented distribution along continental margins and represent isolated habitats on the vast deep-sea floor (Sibuet and Olu, 1998; Levin, 2005). Main questions about biodiversity patterns, dispersal capabilities and life history of fauna and microbes restricted to these chemosynthetic habitats need to be answered in order to understand the interconnectivity and resilience of these dynamic ecosystems (Tyler and Young, 1999; Pradillon *et al.*, 2005, 2007). Moreover, as biodiversity changes over multiple spatial scales (Green and Bohannan, 2006; Ramette and Tiedje, 2007; Martiny *et al.*, 2011; Hanson *et al.*, 2012), a better understanding of the interconnectivity between these fragmented ecosystems needs to be based on quantitative assessments of spatial patterns of species diversity.

Members of the domains Bacteria and Archaea contribute the main functions, that is, hydrocarbon degradation, sulfide production and consumption and chemosynthetic CO_2 fixation (Jørgensen and Boetius, 2007) at cold seep and at other types of chemosynthetic ecosystems. The prevailing energy sources at seeps select for specific types of bacteria and their metabolic functions (Knittel and Boetius, 2009; Goffredi and Orphan, 2010), which differ from those of the surrounding oligotrophic, particle-flux dependent deep-sea ecosystem (Orcutt *et al.*, 2011; Quaiser *et al.*, 2011). But still little quantitative information is available about the similarity and spatial variation of bacterial communities at cold

Correspondence: P Pop Ristova or A Boetius, MARUM—Centre for Marine Environmental Science, University of Bremen, Leobener Strasse, Bremen 28359, Germany.
E-mails: pristova@marum.de or antje.boetius@awi.de
Received 28 May 2014; revised 9 October 2014; accepted 10 October 2014; published online 12 December 2014

seeps (Pop Ristova *et al.*, 2012) and at other types of chemosynthetic ecosystems (Huber *et al.*, 2007; Bienhold *et al.*, 2013), as compared with the deep-sea floor (Jacob *et al.*, 2013 and references therein). At the global scale, it was shown that chemosynthetic ecosystems displayed the highest heterogeneity in bacterial community structure across all oceanic ecosystems (Zinger *et al.*, 2011). Spatial turnover, that is, the relative change in community composition along a spatial gradient (Anderson *et al.*, 2011), of bacterial communities in the deep-sea was previously found to occur not only at large spatial scales in pelagic sediments (>1000s of km; Schauer *et al.*, 2010; Zinger *et al.*, 2011) but also to lesser extent at small scales (<1 km; Pop Ristova *et al.*, 2012; Meyer *et al.*, 2013; Ruff *et al.*, 2013) among reduced habitats of individual systems, mainly due to variations in energy availability and environmental heterogeneity, as well as spatial separation.

Here we investigated bacterial diversity patterns of seep ecosystems of the oligotrophic Eastern Mediterranean deep-sea, with the specific aim to understand how bacterial communities of fragmented, highly reduced sediment habitats vary with spatial scales. Bacterial communities of nine locations distributed over three seep regions were studied using a combined approach, including bacterial community fingerprinting and 454 massively parallel tag sequencing (MPTS), porewater geochemistry, quantification of element fluxes and microbial consumption rates. This allowed for a comparison of microbial diversity at geographical scales ranging from tens of centimeters to hundreds of kilometers. The main aims were to better understand (i) how bacterial communities of reduced methane-seeping habitats compare with those inhabiting surrounding oxidized deep-sea sediments, (ii) which biogeochemical factors shape the bacterial diversity of cold seeps and (iii) if and how bacterial communities of cold seep ecosystems vary with spatial scales.

Material and methods

Description of sampling sites and of analytical procedures

During two consecutive expeditions MSM13/3 and 4 in 2009, on board the RV Maria S Merian, similar types of reduced sediments were sampled from three cold seep regions in the Eastern Mediterranean deep-sea, that is, the Amon Mud Volcano (AMV), the Central Pockmark (Pock) area of the Nile Deep-sea Fan and the Amsterdam Mud Volcano (AmsMV), at depths of 1120–2030 m, located at 128–355 km distance from each other (Table 1, Supplementary Table S1 and Figure 1). In each of the three regions, 2–4 sites were sampled upon visual identification as typical patches of greyish to blackish color, some of which were covered by thin, white thiotrophic bacterial mats (Figure 2b). Geochemically, all seep sites were characterized by methane-seepage and high sulfide concentrations (Table 2). Of these, the AMV_seep_2 samples were obtained from a recently gas-vented seafloor area in the active center of the Amon MV, with not yet fully established active methane-oxidizing community (Felden *et al.*, 2013). Additional non-seep sediment samples were obtained from the immediate vicinity of the cold seep sites (Table 1) and also from distant sites outside of the seepage regions sampled during previous missions (Table 3, also see Supplementary Information).

Total oxygen fluxes and methane effluxes were determined *in situ* with a remotely operated vehicle (ROV QUEST, Marum, Bremen, Germany) benthic chamber module, in which changes in solute concentrations were monitored with an oxygen optode (Aanderaa, Bergen, Norway) and a preprogrammed syringe system sampling bottom waters for methane concentrations (Felden *et al.*, 2013 and references therein). A deep-sea modular microprofiler was used to carry out high-resolution (200 μm) microsensor measurements of oxygen concentrations and to calculate diffusive oxygen uptakes, as described elsewhere (Glud *et al.*, 2009). Total numbers of single cells (1-cm resolution, about 20-cm sediment depth) were determined by applying the acridine orange direct count method according to Boetius and Lochte (1996). Porewater was extracted at a resolution of 1 cm using the Rhizon moisture samplers (Seeberg-Elverfeldt *et al.*, 2005; pore size 0.1 μm), and subsamples were immediately fixed for different types of analyses, that is, NH_4^+, total H_2S, SO_4^{2-}, PO_4^{3-}, dissolved inorganic carbon (DIC) and alkalinity, in the home laboratory. Sulfate reduction (SR) rates were determined *ex situ* by the whole-core injection method with a $^{35}SO_4$ radiotracer (Kallmeyer *et al.*, 2004; Felden *et al.*, 2010). Detailed description of all analytical procedures can be found in the Supplementary Information. All biogeochemical data are available open access via the PANGAEA database (Pop Ristova *et al.*, 2014; http://doi.pangaea.de/10.1594/PANGAEA.830241).

Bacterial community structure at seep and nearby non-seep sites was assessed with automated ribosomal intergenic spacer analysis (ARISA; 1-cm layers, 5-cm sediment depth). In short, DNA was amplified in triplicates with the ITSR and HEX-labeled ITSF primers (Cardinale *et al.*, 2004), targeting the internal transcribed spacer region as described elsewhere (Pop Ristova *et al.*, 2012, also see Supplementary Information). In addition, bacterial communities of seep sites were analyzed by 454 MPTS of the V4–V6 region of the 16 S rRNA gene (10-cm sediment depth) from the same DNA extracts, using the 518 F and 1064 R primers, and following the protocols published on http://vamps.mbl.edu. Data were processed with *mothur* (v.1.29) following the standard operating procedure (Schloss *et al.*, 2009; also see Supplementary Information for detailed information).

Table 1 Overview of the main sampling sites investigated in this study

Cold seep	*Location*	*Habitat*	*Sampling site ID*	*Longitude; latitude*	*Sampling time*
Amon MV (AMV; water depth 1120 m)	Center	Reduced sediment with bacterial mat	AMV_seep_1	32°22.132272'N 31°42.654951'E	October–November 2009
		Reduced sediment	AMV_seep_2	32°22.174029'N 31°42.627174'E	October–November 2009
	Sulfur band	Reduced sediment with bacterial mat (M14 marker)	AMV_seep_3	32°22.045089'N 31°42.276642'E	October–November 2009
		Reduced sediment with bacterial mat (M16 marker)	AMV_seep_4	32°22.045956'N 31°42.265083'E	October–November 2009
		Beige non-seep sediment	AMV_non-seep_1	32°22.3002'N 31°41.9598'E	October–November 2009
Amsterdam MV (AmsMV; water depth 2030 m)		Reduced sediment (M5 marker)	AmsMV_seep_1	35°20.034018'N 30°16.167342'E	November–December 2009
		Reduced sediment (M6 marker)	AmsMV_seep_2	35°20.079390'N 30°16.129803'E	November–December 2009
	Center	Reduced sediment (M10 marker)	AmsMV_seep_3	35°19.945893'N 30°16.098681'E	November–December 2009
	E Rim	Beige non-seep sediment	AmsMV_non-seep_1	35°19.9602'N 30°16.8198'E	November–December 2009
	NE-E Rim	Beige non-seep sediment	AmsMV_non-seep_2	35°20.2398'N 30°17.2902'E	November–December 2009
	Center	Beige seep-influenced non-seep sediment	AmsMV_non-seep_3	35°20.0598'N 30°16.1202'E	November–December 2009
Pockmark (Pock; water depth 1690 m)		Bacterial mat at marker M10	Pock_seep_1	32°31.99'N 30°21.12'E	November–December 2009
		Bacterial mat at marker M9	Pock_seep_2	32°31.98'N 30°21.15'E	November–December 2009
		Beige seep-influenced non-seep sediment	Pock_non-seep_1	32°32.07'N 30°21.39'E	November–December 2009

Detailed list of all samples and measurements performed at each sampling sites are shown in Supplementary Table S1. Physical markers (M) were deployed at almost all the investigated habitats for easier visual recognition.

SFF files of all sequence data have been submitted to the GenBank Sequence Read Archives (http://www.ncbi.nlm.nih.gov) under BioProject ID: PRJNA244496. For the comparison of the community composition of seep regions (V4–V6-based sequences) to non-seep regions (V6-based sequences), only the V6 hypervariable region was compared, and data sets were processed together using the *mothur* (see Supplementary Information for detailed information). Comparability between the derived V6-excised and the original data set was high and significant at the level of beta-diversity (change in community structure between sites), Shannon diversity index and the taxonomical level of class (Supplementary Table S2 and Supplementary Figures S1–S3).

Statistical analyses. ARISA peaks were binned (2-bp bin size; Interactive Binner function, http://www.ecology-research.com; Ramette, 2009), and ARISA PCR triplicates were merged into a consensus profile by keeping only operational taxonomic units (OTU) that appeared in at least two of the PCR replicates and by averaging the corresponding relative peak intensities. 454 MPTS sequences were clustered at 97% sequence's similarity level ($OTU_{0.03}$). Singletons were counted as $OTU_{0.03}$ represented by only one sequence in the whole data set. Shannon diversity index was used to compare the diversity of seep and non-seep regions, as this index was shown to be reliable and stable across studies and data sets based on different primer sets (He *et al.*, 2013). Additionally, variations in the diversity of seep sites were compared by calculating the Chao1 and ACE richness estimates (same primer set). For both analyses, sample diversity was calculated on normalized 454 MPTS subset based on the sample with the least number of sequences (Pock_seep_2, 7925), using *mothur*

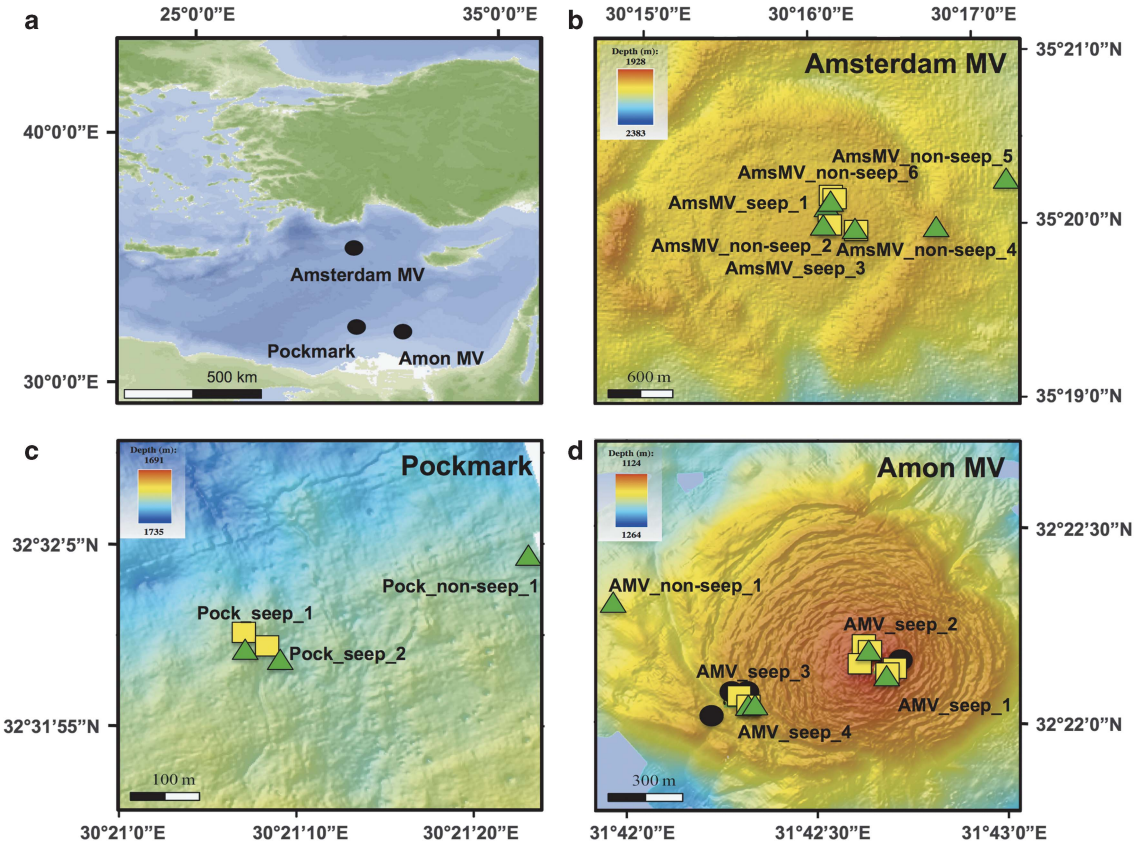

Figure 1 Overview maps of all three investigated cold seep regions, including seep and non-seep sites in the Eastern Mediterranean Sea (**a**) the Amsterdam MV (**b**), the Pockmark area (**c**), and Amon MV (**d**). The main sampling and measurement sites are depicted with symbols, that is, push core and multicore sampling (green triangles), benthic chamber incubations (yellow squares) and microprofiler measurements (black circles).

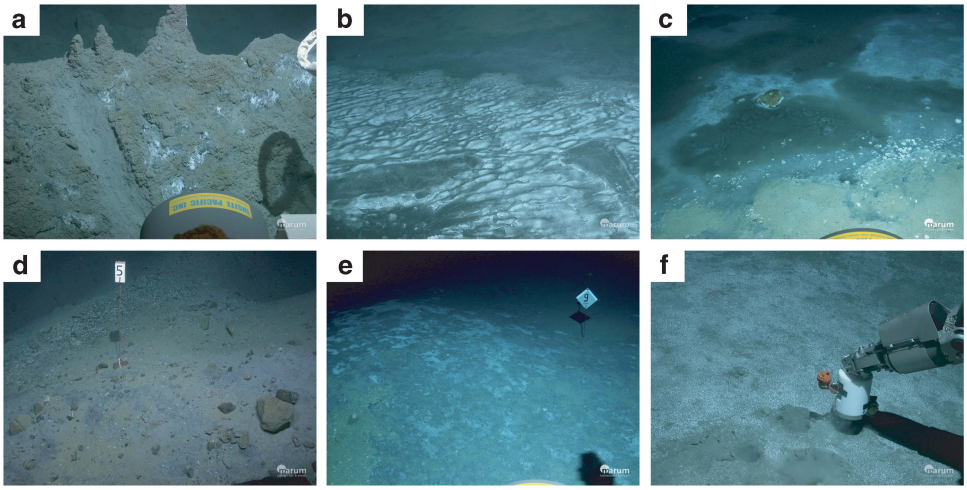

Figure 2 Underwater photographs of reduced seep habitats investigated in this study: Upper panel (**a**, **b**, **c**) photographs were taken at the Amon MV and lower panel (**d**) photographs at the Amsterdam MV and (**e**, **f**) at a Pockmark seep. (**a**) Center of the Amon MV characterized by gassy sediments and patchy bacterial mats, (**b**, **c**) a lateral mud flow with extensive bacterial mats at the outer rim of the volcano. (**d**) Typical methane-seeping habitat marked by black sediment patches encountered at the Amsterdam MV. Overview (**e**) and a more detailed photo (**f**) of a bacterial mat habitat at the Pockmark cold seep.

v.1.29.1 (Schloss *et al.*, 2009). Percentage of shared OTUs was calculated by pairwise comparison to assess similarity between sites at small (<10 cm; within individual sites), intermediate (50–630 m, between sites within one cold seep region) and large spatial scales (128–355 km, between sites of different cold seep regions). All statistical analyses were performed in the R statistical computing language

Table 2 Biogeochemical characterization of seep and nearby non-seep sites, including average depth integrated (0–10 cm) sulfate reduction (SR) rates, total oxygen uptake (TOU), methane efflux, diffusive oxygen uptake (DOU), oxygen penetration depth (OPD), minimum detected concentration of sulfate and sulfate penetration depth

Cold seep	*Sampling site*	*SR* $mmol\,m^{-2}\,d^{-1}$	*TOU* $mmol\,m^{-2}\,d^{-1}$	*CH_4 efflux* $mmol\,m^{-2}\,d^{-1}$	*DOU* $mmol\,m^{-2}\,d^{-1}$	*OPD* mm	*Min. SO_4* $mmol\,l^{-1}$	*SO_4 depth* cm
Amon MV	AMV_seep_1	16	115	83; 85; 49	47	2	<1	10
	AMV_seep_2	2	5	1; 70; 24	11	3	29	>19
	AMV_seep_3	28	119	<1	3; 6	1; 3.9	<1	5
	AMV_seep_4	1	13	ND	5	45	29	>18
Amsterdam MV	AmsMV_seep_1	35	101	1175	ND	ND	<1	15
	AmsMV_seep_2	8	23	196	ND	ND	4	>15
	AmsMV_seep_3	13	89	1169	ND	ND	<1	8
Pockmark	Pock_seep_1	20	153	688	ND	ND	<1	12
	Pock_seep_2	50	228	36	ND	ND	1	20
Amon MV	AMV_non-seep_1	0[a]	5[a]	ND	12[a]	>40[a]	29[b]	>13[b]
Amsterdam MV	AmsMV_non-seep_1	0	ND	ND	ND	ND	27	>30
	AmsMV_non-seep_2	1	ND	ND	ND	ND	28	>25
	AmsMV_non-seep_3	56	ND	ND	ND	ND	27	>17
Pockmark	Pock_non-seep_1	0	1[a]	ND	0.5[a]	>10[a]	27	>29

Abbreviation: ND, not detected. For further details on the Amon MV biogeochemistry, see Felden *et al.* (2013).
Intermediate sites with subsurface seepage include AMV_seep_4 and AmsMV_non-seep_3.
[a]Grünke *et al.*, 2011.
[b]Data derived from M70/2a cruise.

Table 3 454 MPTS—derived sample characteristics and species richness estimates

Sample ID	*Number of sequences*	*Number of $OTU_{0.03}$*	*Number of $OTU_{0.03}$ singletons*	*Relative number of $OTU_{0.03}$ singletons (%)*	*Chao1*	*ACE*	*Shannon index*
AMV_seep_1	10988	1478	700	47	3592	6794	5.6
AMV_seep_3	9062	1892	1073	57	6164	11943	5.5
AMV_seep_4	11661	2250	1198	53	5041	9526	6.1
AmsMV_seep_1	9929	1216	451	37	2863	4780	5.1
AmsMV_seep_2	8598	1192	460	39	3047	6060	4.9
AmsMV_seep_3	13186	1487	623	42	2793	4833	5.0
Pock_seep_1	15774	1640	740	45	3015	5778	5.1
Pock_seep_2	7925	1023	418	41	3120	5919	5.0
Emed_non-seep_region_1[a]	19369	1535	527	34	ND	ND	5.3
Emed_non-seep_region_2[a]	27606	2280	864	38	ND	ND	5.2
Emed_non-seep_region_3[a]	15422	1522	538	35	ND	ND	6.0

Abbreviations: ND, not determined; OTU, operational taxonomic unit.
Three regions without cold seep systems (Emed_non-seep_region_1–3) were included to test for differences in biodiversity at larger distances.
[a]Sediment samples from non-seep regions were taken at 1375–2968 m water depth in the deep Eastern Mediterranean Sea (Boetius and Lochte, 1996).

(v.2.15), using *vegan* (Oksanen *et al.*, 2011) and *labdsv* (Roberts, 2013). Indicator taxa characterizing each cold seep structure were identified via indicator species analysis according to Dufrêne and Legendre, (1997). Dissimilarity matrices based on community (pooled ARISA replicates or 454 MPTS) and on porewater data (DIC, H_2S and SO_4) were calculated using Bray–Curtis and Euclidean distances, respectively. For all analyses, ARISA profiles of individual depth sediment layers were pooled *in silico*, except for the analyses of correlation between diversity and porewater geochemistry, as well as investigation of bacterial community structure of seep and non-seeps. Community differences were visualized with non-metric multidimensional scaling analyses and tested for significance using the analysis of similarity test. Mantel test with 999 Monte-Carlo permutations was used to test for significance of Spearman and Pearson correlations between community and environmental (for example, differences in porewater concentrations) distance matrices. Mantel *P*-values were corrected for multiple testing using the Bonferroni's correction (Ramette, 2007).

Results

Geochemical characterization of seep versus non-seeps habitats

At all three cold seep systems, the Amon Mud Volcano (AMV), Amsterdam Mud Volcano (AmsMV) and the Pockmark area (Pock), we sampled visually and biogeochemically distinct patches of highly reduced, methane-seeping sulfidic sediments of dark grey to blackish color, which were separated by non-reduced oxygenated seafloor areas (Figure 1).

The areas directly surrounding the reduced patches consisted of beige sediments, showed little to no influence of methane seepage and were sampled as 'non-seep sites'. Microsensor measurements confirmed that all non-seep sites were fully oxygenated until the penetration depth of the sensors (>1–4 cm sediment depth) (Figure 3f). Throughout the top 20 cm, these had sulfate and DIC porewater concentrations of 28 and 2.3 mmol l^{-1}, respectively, reflecting bottom water concentrations (Table 2, Supplementary Figures S4 and S5). AMV_seep_4 and AmsMV_non-seep_3 were intermediate sites with some signs of subsurface seepage. Total oxygen uptake (TOU) and diffusive oxygen uptake were low (1–12 mmol m^{-2} d^{-1}), and SR rates barely detectable (Table 2, Supplementary Figure S6). Ammonium and phosphate concentrations in the porewaters were also low, with, on average, 2 μmol l^{-1} and 1 μmol l^{-1}, respectively (Supplementary Figure S7). Elevated NH_4^+ and subsurface SR rates measured at AmsMV_non-seep_3 indicate horizontal methane migration, placing this sample biogeochemically between a seep and a non-seep site. At all non-seep sites, cell numbers of 0.2–1.7 × 10^9 cm^{-3} were detected in the top 5-cm surface layers, as well as a decline with sediment depth (Supplementary Figure S8).

Seepage of dissolved methane to the bottom water was detected at all seep sites, with maximum effluxes of 1169 and 1175 mmol m^{-2} d^{-1} measured at two of the Amsterdam MV sites (Table 2). Methane efflux measured at the AMV_seep_2 site varied between 1 and 70 mmol m^{-2} d^{-1} within days of sampling, reflecting high temporal and/or spatial variations in the seepage of methane at this location. At most of the seep sites, oxygen penetration was limited to the topmost 0.4 cm of sediment (Figure 3c), except at the AMV_seep_4 where oxygen was detected down to 4 cm depth (Table 2). Diffusive oxygen flux was elevated at all seep sites compared with the non-seep sites and reached a maximum value of 47 mmol m^{-2} d^{-1} at the AMV_seep_1 site. Both Pockmark sites had the highest benthic TOU (153 and 228 mmol m^{-2} d^{-1}) detected in this study. All other investigated seep sites had more variable TOU (5–119 mmol m^{-2} d^{-1}; Table 2).

Integrated (0–10 cm) SR rates at seep sites showed similar patterns as TOU, with the highest rates detected in the Pockmark region (20 and 50 mmol m^{-2} d^{-1}), while the other sites had more variable sulfate consumption (1–35 mmol m^{-2} d^{-1}; Table 2). Concentrations of total sulfide were elevated (max. 24 mmol l^{-1}) at all seeps and increased with sediment depth, except at two of

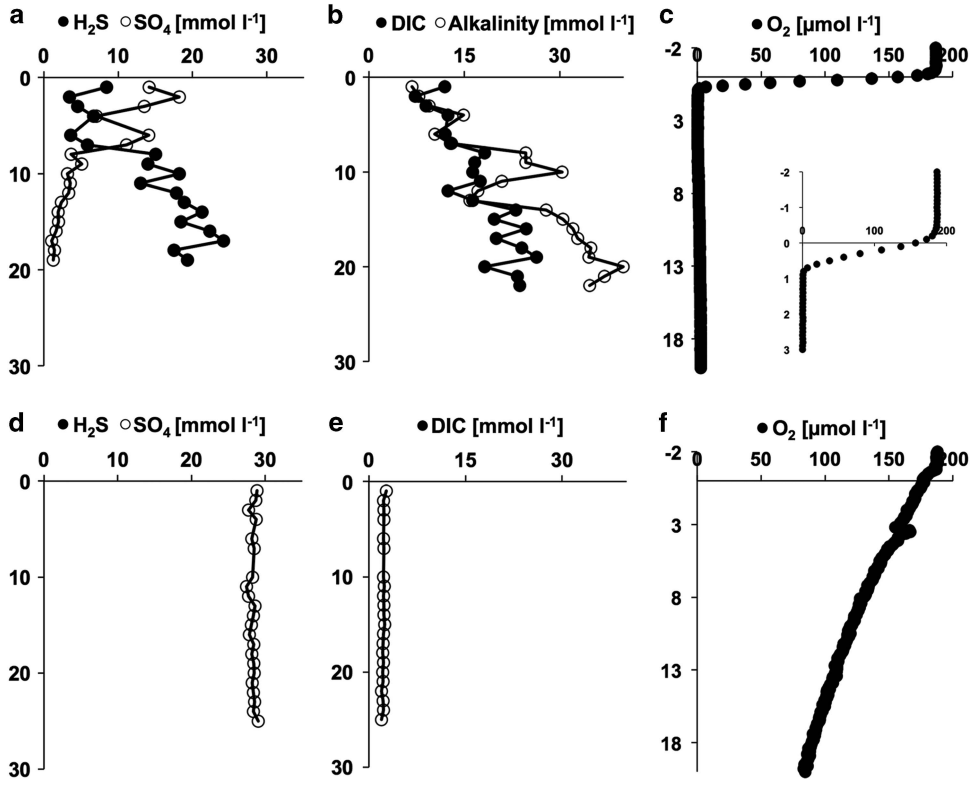

Figure 3 Plots of porewater concentration profiles at methane-seeping, reduced sites (**a–c**; Pock_seep_1) and at nearby non-seep sites from the Pockmark region (**d–f**; Pock_non-seep_1). (**a**, **d**) Depth profiles of total sulfide (closed circles) and sulfate concentrations (open circles); (**b**, **e**) DIC concentration (open circles) and alkalinity (closed circles); (**c**, **f**) *in situ* oxygen concentration determined with microsensors, the insert in panel (**c**) shows the same profile at higher depth resolution. Further detailed geochemistry plots of all regions can be found in the Supplementary Figures S1–S5.

the Amon MV sites (AMV_seep_2 and AMV_seep_4) where no free sulfide was detected throughout the complete investigated sediment depth (Figure 3a, Supplementary Figure S4). At all other seep sites, sulfate concentration profiles steeply decreased with depth, and sulfate was often completely consumed (Table 2). Alkalinity and DIC concentrations were substantially elevated (max. 33–37 mmol l^{-1}) and increased with depth, except at the AMV_seep_2 and AMV_seep_4 where background values (2.4 mmol l^{-1}) were measured through the complete core depth (Figure 3b, Supplementary Figure S5). Ammonium concentrations varied substantially between different sites and mainly increased with sediment depth, to reach a maximum value of 4.4 mmol l^{-1} at the AMV_seep_3 (Supplementary Figure S7). Phosphate concentrations (average 3 μmol l^{-1}) were similar at all seeps, exceeding those of non-seep sites. All of the seeps, except AMV_seep_2, had higher bacterial cell numbers compared with the non-seep sites, with maximum values of 0.3–6.7 × 10^9 cm^{-3} in the topmost 5-cm sediment depth. Differences in the cell numbers between non-seeps and seeps (excluding the newly formed AMV_seep_2 site) were statistically significant (Mann–Whitney $W=30$, $P=0.01$). Cell numbers at all seeps declined with sediment depth to reach 0.1 × 10^9 cm^{-3} at 15 cm (Supplementary Figure S8).

Comparison of bacterial communities between seep and non-seep regions

The Shannon diversity index did not differ between seep regions (5.3 ± 0.4 s.d., $n=8$) and non-seep regions of the Eastern Mediterranean Sea (5.5 ± 0.5 s.d., $n=3$; Mann–Whitney $W=7$, P-value = 0.4; Table 3). Within the seep regions, observed ARISA OTU numbers were also not different between methane-seeping sites (241 ± 31 s.d., $n=9$) and non-seeping sites (212 ± 55, $n=5$; Mann–Whitney $W=28$, $P=0.5$).

Pairwise comparison of methane-seeping sites and the corresponding nearby non-seeping sites (0.01–1.8 km apart) revealed that, on average, between all pairs only 36% of the ARISA OTUs were shared (Supplementary Table 5a). Overall, seep and non-seep sites shared only 18% of a total of 158 ARISA OTUs and had communities with significantly different structures (analysis of similarity $R=0.8$, Bonferroni's $P=0.001$; Figure 4).

Pooled 454 sequences of all seep sites were dominated by *Deltaproteobacteria* (26%), *Gammaproteobacteria* (17%), *Anaerolineae* (11%), *Epsilonproteobacteria* (7%) and *Caldilineae* (7%) (Table 4). In contrast, most abundant taxa of Eastern Mediterranean deep-sea sediments from non-seep regions were dominated by *Betaproteobacteria* (17%), *Gammaproteobacteria* (14%), *Synergistia* (12%), *Alphaproteobacteria* (8%) and *Flavobacteria* (8%). Furthermore, the relative sequence abundance

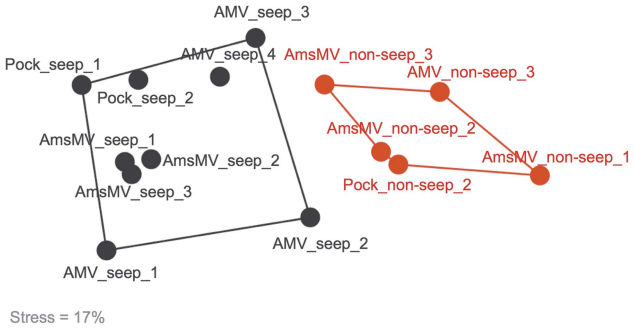

Figure 4 Non-metric multidimensional scaling analysis depicting differences in the bacterial community structure between seep (black symbols) and non-seep sites (red symbols) of three cold seep regions, as derived from ARISA-based data. Convex hulls depict significant differences between the groups, as determined by analysis of similarity ($R=0.8$, Bonferroni's $P=0.001$). Pooled (0–5 cm) samples per site were used to calculate Bray–Curtis dissimilarity matrix.

of the *Epsilonproteobacteria*, encompassing many types of microbes that gain energy via oxidation of sulfide, differed between seep (7% of all sequences) and non-seep regions (1%) (Table 4). Among the three most abundant $OTU_{0.03}$ in the whole seep data set, two belonged to *Epsilonproteobacteria* and were closely related to sulfide-oxidizing *Sulfurovum*. Putative sulfur reducers and oxidizers of the *Desulfobacteraceae*, *Desulfobulbaceae*, *Thiotrichales* and *Acidithiobacillales*, along with aerobic methane oxidizers of the *Methylococcus*, were the most abundant microorganisms within the *Deltaproteobacteria* and *Gammaproteobacteria* at all seep sites (Supplementary Table S3). At non-seep regions, facultative anaerobic heterotrophs of the *Alteromonadales* and *Oceanospirillales*, as well as *Desulfobacteraceae* and *Desulfobulbaceae*, were the most abundant taxa within the *Gammaproteobacteria* and *Deltaproteobacteria*, respectively.

Bacterial communities of cold seeps and factors shaping their structure

Among the seep sites, the richness estimates varied twofold (2793–6164 Chao1 index). Highest variation in the estimated richness existed between seep sites of the Amon MV (Table 3). Samples of this MV had significantly higher estimated richness than the Pockmark and Amsterdam MV samples (Mann–Whitney $W=15$, $P=0.04$. Similar patterns were obtained when using ARISA OTUs instead (Supplementary Figure S9).

The majority of $OTU_{0.03}$ (32%) occurred at only 1–2 sites, and only 92 of the total 8117 $OTU_{0.03}$ (that is, 4% of all types, excluding singletons) were common to all seep sites and comprised the core seep community with 59% of all sequences (Supplementary Figure S10). Most of the core $OTU_{0.03}$ were affiliated to *Deltaproteobacteria* (23%), *Caldilineae* (14%), *Gammaproteobacteria* (11%), *Anaerolineae* (11%), *Sphingobacteria* (8%) and *Epsilonproteobacteria* (5%) (Supplementary

Table S4). The three different cold seep regions had significantly different community structures (analysis of similarity $R = 0.3–0.6$, Bonferroni's $P \leqslant 0.003$, Figure 5c), and only the AMV_seep_1 showed higher similarity to the Amsterdam MV samples (Figures 5a and b). Indicator species analysis revealed that most indicator $OTU_{0.03}$ of Amon and Amsterdam MV belonged to the class of *Deltaproteobacteria* and *Gammaproteobacteria*. The Pockmark sites had no unique $OTU_{0.03}$ in the *Gammaproteobacteria* but in the *Anaerolineae*, *Epsilon-* and *Deltaproteobacteria*.

Sample diversity of seep habitats was inversely related to seepage activity, as revealed by the significant negative correlation between CH_4 effluxes and Chao1 and ACE estimated richness (Spearman's coefficient $R = -0.9$, $P \leqslant 0.01$). No significant correlation between beta-diversity (full 454 data set or only *Deltaproteobacteria* sequences) with seep activity, defined as SR, TOU or CH_4 efflux, could be observed (Mantel test $R < 0.05$, $P > 0.4$). On the other hand, beta-diversity based on ARISA (data set, including all sites and sediment depth layers) was significantly and positively correlated with differences in porewater concentrations of sulfide, DIC and sulfate between seep sites ($R = 0.5–0.3$, Bonferroni's $P = 0.01–0.04$; Figure 6).

Spatial variations of seep-influenced bacterial communities

Pairwise analyses based on shared ARISA or 454 OTUs revealed decreasing similarity between samples with increasing distance for seep and non-seep sites within the scale of 0–350 km investigated here. On the smallest investigated spatial scale (<10 cm; within site comparison), a pair of samples shared, on average, 76% OTUs for seep (±4% s.d., $n = 9$)

Table 4 Ten most sequence-abundant bacterial classes

AMV_seep_1	*AMV_seep_3*	*AMV_seep_4*	*AmsMV_seep_1*	*AmsMV_seep_2*	*AmsMV_seep_3*
Deltaproteobacteria (36)	Deltaproteobacteria (36)	Deltaproteobacteria (22)	Deltaproteobacteria (30)	Deltaproteobacteria (27)	Deltaproteobacteria (30)
Epsilonproteobacteria (16)	Anaerolineae (17)	Gammaproteobacteria (18)	Gammaproteobacteria (16)	Gammaproteobacteria (18)	Gammaproteobacteria (16)
Anaerolineae (11)	Caldilineae (12)	Anaerolineae (16)	Anaerolineae (15)	Anaerolineae (8)	Epsilonproteobacteria (10)
Gammaproteobacteria (11)	Gammaproteobacteria (6)	Caldilineae (10)	Sphingobacteria (5)	Epsilonproteobacteria (7)	Anaerolineae (7)
Sphingobacteria (5)	Epsilonproteobacteria (4)	Epsilonproteobacteria (5)	Caldilineae (4)	Milano-WF1B-44 (7)	Flavobacteria (5)
Holophagae (2)	Phycisphaerae (2)	Holophagae (3)	Milano-WF1B-44 (4)	Sphingobacteria (5)	Sphingobacteria (4)
Clostridia (2)	Sphingobacteria (2)	Milano-WF1B-44 (2)	Holophagae (2)	Flavobacteria (5)	Milano-WF1B-44 (4)
Caldilineae (2)	Clostridia (1)	Actinobacteria (2)	Actinobacteria (2)	Caldilineae (4)	Clostridia (4)
Actinobacteria (1)	Actinobacteria (1)	Sphingobacteria (2)	Epsilonproteobacteria (2)	Holophagae (3)	Caldilineae (2)
Flavobacteria (1)	Holophagae (1)	Flavobacteria (1)	Clostridia (2)	Actinobacteria (2)	Holophagae (2)
Pock_seep_1	*Pock_seep_2*	*Emed_non-seep_region_1*	*Emed_non-seep_region_2*	*Emed_non-seep_region_3*	
Deltaproteobacteria (30)	Deltaproteobacteria (29)	Betaproteobacteria (19)	Betaproteobacteria (18)	Betaproteobacteria (12)	
Epsilonproteobacteria (25)	Anaerolineae (26)	Gammaproteobacteria (16)	Synergistia (16)	Gammaproteobacteria (12)	
Anaerolineae (16)	Epsilonproteobacteria (12)	Synergistia (12)	Flavobacteria (15)	Alphaproteobacteria (12)	
Caldilineae (6)	Caldilineae (10)	Actinobacteria (9)	Gammaproteobacteria (14)	Actinobacteria (10)	
Sphingobacteria (4)	Sphingobacteria (4)	Deltaproteobacteria (6)	Alphaproteobacteria (8)	Deltaproteobacteria (7)	
Gammaproteobacteria (3)	Gammaproteobacteria (3)	Alphaproteobacteria (6)	Deltaproteobacteria (6)	Bacilli (6)	
Clostridia (1)	Milano-WF1B-44 (2)	Acidobacteria (6)	Actinobacteria (4)	Acidobacteria (4)	
Phycisphaerae (1)	Holophagae (1)	Bacilli (3)	Sphingobacteria (3)	SAR202 (3)	
Holophagae (1)	Actinobacteria (1)	ML635J-21 (3)	Bacilli (2)	Synergistia (2)	
Milano-WF1B-44 (1)	Phycisphaerae (1)	Holophagae (3)	Clostridia (2)	Holophagae (2)	

The relative percentage of sequence abundance for each seep site is given in parentheses. For comparison, three samples from non-seep regions of the deep Eastern Mediterranean sea were included.

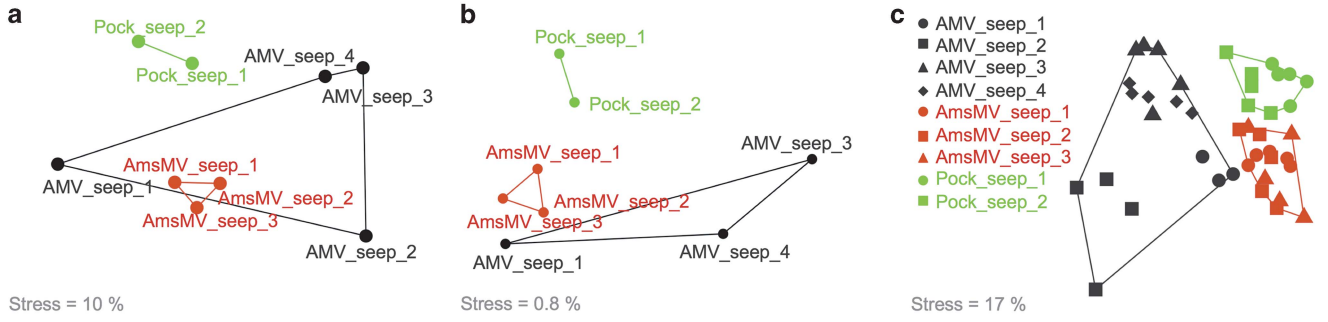

Figure 5 Non-metric multidimensional scaling analysis plots (based on Bray–Curtis dissimilarity) depicting differences in the bacterial community structure between different seep regions, as calculated from depth-pooled ARISA (**a**) and 454 MPTS (**b**), as well as depth-unpooled ARISA data (**c**). Seep sites are colored according to the seep region: Amsterdam MV sites in red, Amon MV sites in black, and Pockmark sites in green. Different sites within the same seep region are depicted with different symbols. Convex hulls in (**c**) depict significant differences between the groups, as determined by analysis of similarity ($R = 0.3–0.6$, Bonferroni's $P \leqslant 0.003$).

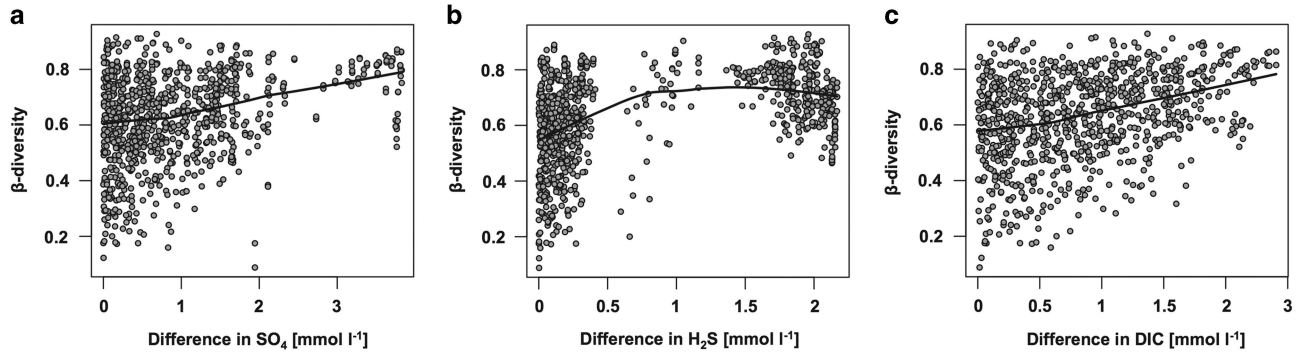

Figure 6 Plot depicting positive relation between beta-diversity (derived from ARISA) and differences in sulfate (**a**), sulfide (**b**) and DIC concentrations (**c**). Solid line represents a *LOWESS* curve (locally weighted scatterplot smoothing).

and non-seep sites (±8% s.d., $n=5$). The sharpest decrease in the percentage of shared ARISA OTUs (54±8% s.d., $n=3$) was evident at intermediate spatial scales (20–630 m; between sites within one region), after which on the largest spatial scales (100 s of km; between cold seep regions) the trend leveled off at 51% shared OTUs for non-seep ($n=2$) and 52% (± 3% s.d.; $n=3$) for seep samples (Supplementary Table S5a). Pairwise comparison based on the 454 MPTS data set revealed a similar pattern but with lower values (Supplementary Table S5b). Accordingly, species accumulation analyses showed a linear increase, without reaching a plateau, in $OTU_{0.03}$ diversity with increasing number of seep samples considered (Figure 7).

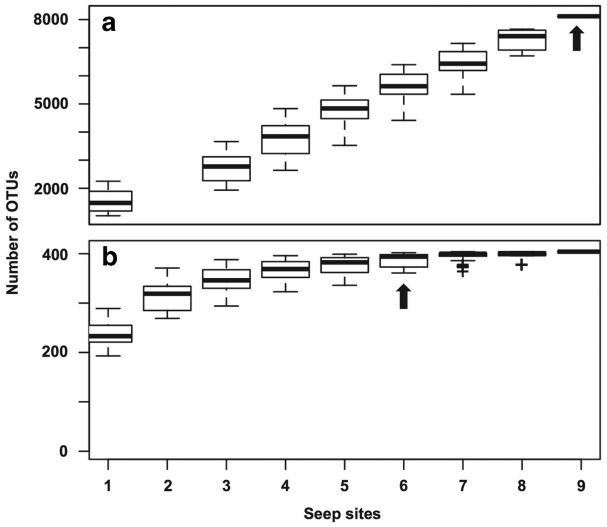

Figure 7 OTU accumulation curves, based on the 454 MPTS (**a**) and ARISA (**b**) data. Arrow indicates the number of seep sites needed to recover 95% of the observed OTUs.

Discussion

Cold seeps as islands with distinct microbial communities at the deep-sea floor

Previous investigations have indicated that cold seeps host higher biomass and lower diversities of animals than non-seep sediments (reviewed in Levin, 2005). As to microbial diversity, it was suggested that extreme environments in general host less diverse microbial communities than more stable, homogenized environments (Frontier, 1985). Results of this study reveal that cold seep habitats have similar levels of bacterial diversity (determined as Shannon index; Table 3) and host significantly higher cell numbers compared with typical oxygenated sediments in the oligotrophic deep Eastern Mediterranean. In line with this finding, but using other methods, it was previously shown that other cold seeps in the Eastern Mediterranean harbor similar bacterial diversity to background sediments with no sulfide production (Heijs *et al.*, 2008).

Investigation of the whole community structure using high-resolution fingerprinting techniques revealed that communities of seep sediments in the Eastern Mediterranean deep-sea differed also in their composition and relative abundance compared with adjacent and distant non-seep sediments. This expands the findings of previous studies, which have identified differences in the presence and proportion of key functional groups of the *Deltaproteobacteria*, *Gammaproteobacteria* and *Epsilonproteobacteria* involved in aerobic and anaerobic hydrocarbon degradation, as well as sulfur cycling (Orphan *et al.*, 2001; Knittel *et al.*, 2003; Heijs *et al.*, 2008; Orcutt *et al.*, 2011; Ruff *et al.*, 2013). Differences were also found at the level of the whole community between seep and non-seep regions, for example, by the high sequence abundances of the chemo-organotrophic *Anaerolineae* and *Caldilineae* of the *Chloroflexi* at seeps and their virtual absence in non-seep sediments (Table 4; Polymenakou *et al.*, 2005). In line with our results, it was previously found in the Pacific that deep-biosphere hydrate-bearing sediments harbor distinct bacterial communities compared with hydrate-free sites (Inagaki *et al.*, 2006). Hence, at the level of beta-diversity, bacterial community patterns match those of seep animals (Sahling *et al.*, 2002; Levin *et al.*, 2003, 2010; Olu *et al.*, 2009; van Gaever *et al.*, 2009; Menot *et al.*, 2010; Ritt *et al.*, 2011), in that their community structures differ significantly from background communities colonizing deep-sea sediments.

Seep sites harbor distinct bacterial communities when compared with nearby non-seep sites (<1.8 km), sharing 22–45% of their OTUs with neighboring habitats, and 18% over the complete ARISA data set (Supplementary Table S5). In comparison, at other seep sites at the northeastern Pacific margin macrofauna communities were found to share a much higher proportion of species between seep and non-seep sites (Levin *et al.*, 2010). High adaptation of communities to their respective environments and different types of energy sources, as well as the variable tolerance to toxic conditions caused by sulfide production at cold seeps, are regarded as main factors selecting for different macrofaunal communities at seep and non-seep sites (Sibuet and Olu, 1998; Levin *et al.*, 2010). The same proposed factors and mechanisms could be also responsible for the differences in the bacterial communities of seeps and non-seeps observed here, but further studies are necessary to determine this relationship.

Factors shaping the bacterial diversity at cold seep ecosystems

Cold seeps are highly heterogeneous ecosystems (Cordes *et al.*, 2010), with patchy emission pathways of the main sources of energy—methane, other hydrocarbons and sulfide (Barry *et al.*, 1997; de Beer *et al.*, 2006; Omoregie *et al.*, 2009; Treude *et al.*, 2009; Pop Ristova *et al.*, 2012). Accordingly, only few bacterial groups were found in common to all the investigated cold seeps, of which sulfate reducers belonging to the *Desulfobacteraceae* and *Desulfobulbaceae*, as well as sulfide oxidizers *Helicobacteraceae*, were the most abundant and diverse taxa (Supplementary Table S4). Hence we propose that microorganisms affiliated to these families can be regarded as bacterial indicators of seep ecosystems, with overlaps to whale and wood falls (Bienhold *et al.*, 2013). Previous studies have identified differences in the distribution of key functional groups of the *Deltaproteobacteria*, *Gammaproteobacteria*and *Epsilonproteobacteria* involved in hydrocarbon degradation and sulfur cycling in relation to environmental features (Orphan *et al.*, 2001; Knittel *et al.*, 2003; Heijs *et al.*, 2008; Orcutt *et al.*, 2011; Ruff *et al.*, 2013). At the level of the bacterial community structure, patterns could be related to contrasting local geochemical conditions within one seep structure (Omoregie *et al.*, 2008; Grünke *et al.*, 2011; Pop Ristova *et al.*, 2012). In this study, bacterial communities were compared across a range of different biogeochemical activities related to seepage (Table 2). Bacterial communities exhibited a patchy distribution from local to regional scales and increasing dissimilarity with increasing difference in seep sediment geochemistry (Figures 5 and 6). Similarity among seep sites was high at the level of bacterial classes, but seep habitats differed substantially regarding their relative abundance and composition at the $OTU_{0.03}$ level (Table 4). The highly dynamic Amon MV system (Felden *et al.*, 2013) with very different types of seep settings—that is, gas versus brine driven fluid flow—showed significantly higher bacterial richness and variability compared with the Pockmark and Amsterdam MV sites (Table 3, Figures 5a–c). Underlying seep geochemistry was responsible for shaping both the alpha- and beta-diversity of cold seeps. Positive relationships between richness and energy availability have been revealed for other marine ecosystems (Pommier *et al.*, 2007; Fuhrman *et al.*, 2008; Bienhold *et al.*, 2012). A negative trend revealed here between methane efflux and microbial richness in seeps may be explained by the finding that the highest methane efflux rates came from relatively recent seep sites from within a disturbed mud volcano center (Felden *et al.*, 2013). Non-metric multidimensional scaling analyses based on a subset of the community, including only classes such as *Deltaproteobacteria*, *Gammaproteobacteria*, *Epsilonproteobacteria*, *Caldilineae* and *Anaerolineae*, revealed highly similar patterns correlated to those based on the whole bacterial community (Supplementary Table S6). This implies that, in terms of diversification, not only key functional groups involved in hydrocarbon degradation such as methane-oxidizing, sulfur-reducing and -oxidizing microorganisms but also other bacterial types such as the *Chloroflexi* may respond similarly to geochemical variations at cold seep ecosystems. Members of the *Chloroflexi* have been found at cold seeps, deep hydrocarbon-bearing sediments and, in general, organic-rich sediments (Kormas *et al.*, 2003; Inagaki *et al.*, 2006; Pachiadaki *et al.*, 2010), where they comprise high portion of the total bacterial community (30%, this study). The role of this bacterial group at cold seep ecosystems is largely unknown and should be addressed in future studies.

Effect of spatial scales on bacterial diversity of cold seep ecosystems

Knowledge on the biodiversity patterns of deep-sea organisms across space and time is important to anticipate responses of deep-sea ecosystems to current and future environmental and anthropogenic changes (Danovaro *et al.*, 2008, 2010; Levin and Sibuet, 2012). Results of this study show that spatial patterns of bacterial communities of cold seeps comply with the taxa–area relationship, that is, an increase in species richness with increasing size of sampled area (Figure 7). This pattern has been reported for all domains of life and across different habitats, including meiofauna and macrofauna seep organisms (Cordes *et al.*, 2010), and hence is thought to be one of the few universal laws in ecology (Rosenzweig, 1995; Lawton, 1999; Zinger *et al.*, 2014). A general trend of increasing dissimilarities in the bacterial communities with geographic distance has been identified across various ecosystems on large spatial scales (Papke *et al.*,

2003; Whitaker *et al.*, 2003; Martiny *et al.*, 2006; Ramette and Tiedje, 2007; Schauer *et al.*, 2010; Zinger *et al.*, 2014). In our study, the percentage of shared ARISA bacterial types was the highest within sites (76%), substantially declined between sites (54%) and remained at the same level between different cold seep regions (52%) (Supplementary Table S5). Hence, highest spatial turnover occurred on intermediate spatial scales (<1 km), within individual seep regions, among locations spatially separated by few meters to hundreds of meters. With approximately one-third of the microbial diversity being unique to the individual seep habitats, that is, patches of reduced sediments of only a few meters in diameter, these localities significantly contribute to the biodiversity of deep-sea, explaining why cold seep systems can be regarded as biodiversity hotspots. The small, reduced habitats may have a critical role for the connectivity and diversity of margin communities and might provide resilience to perturbations caused by increased anthropogenic impact. This is a relevant finding with regard to spatial management of deep-water ecosystems, such as for deep-sea oil and gas resources; however, this also suggests that cold seep communities could be vulnerable to habitat losses at the scale of the individual seep ecosystem (Ramirez-Llodra *et al.*, 2011; van Dover *et al.*, 2011).

Conflict of Interest

The authors declare no conflict of interest.

Acknowledgements

We thank the crew of RV Maria S Merian and the pilots of ROV Quest (Marum, University Bremen) for their invaluable help during the MSM13/3 and 4 cruises. Christina Bienhold, Viola Beier, Gabriele Schuüssler, Rafael Stiens, Volker Asendorf, Axel Nordhausen, Joürn Patrick Meyer, Wiebke Rentzsch, Erika Weiz, Sebastian Strauß, Christian Quast and Marianne Jacob are gratefully acknowledged for help with onboard and laboratory work and discussions on data analyses. We thank Mitchell Sogin and his team at the MBL (Woods Hole) for 454 sequencing, Gerhard Bohrmann for providing microbathymetry data of the Amsterdam MV (expeditions M70/3 and MSM13/4), and Stefanie Meyer and Paul Wintersteller for help with processing. The research was carried out in the framework of the EC FP7 HERMIONE project (no. 226354) and the DFG Research Center/Cluster of Excellence Marum 'The Ocean in the Earth System' of the University Bremen. We also thank the DFG (MERIAN expeditions) and Leibniz project to AB and the MPG for providing additional funds to the study.

References

Anderson MJ, Crist TO, Chase JM, Vellend M, Inouye BD, Freestone AL *et al.* (2011). Navigating the multiple meanings of beta-diversity: a roadmap for the practicing ecologist. *Ecol Lett* **14**: 19–28.

Barry JP, Kochevar RE, Baxter CH. (1997). The influence of pore-water chemistry and physiology on the distribution of vesicomyid clams at cold seeps in Monterey Bay: implications for patterns of chemosynthetic community organization. *Limnol Oceanogr* **42**: 318–328.

Bienhold C, Boetius A, Ramette A. (2012). The energy-diversity relationship of complex bacterial communities in Arctic deep-sea sediments. *ISME J* **6**: 1–9.

Bienhold C, Pop Ristova P, Wenzhöfer F, Dittmar T, Boetius A. (2013). How deep-sea wood falls sustain chemosynthetic life. *PLoS One* **8**: e53590.

Boetius A, Lochte K. (1996). Effect of organic enrichments on hydrolytic potentials and growth of bacteria in deep-sea sediments. *Mar Ecol Prog Ser* **140**: 239–250.

Boetius A, Wenzhöfer F. (2013). Seafloor oxygen consumption fuelled by methane from cold seeps. *Nat Geosci* **6**: 725–734.

Cardinale M, Brusetti L, Quatrini P, Borin S, Puglia AM, Rizzi A *et al.* (2004). Comparison of different primer sets for use in automated ribosomal intergenic spacer analysis of complex bacterial communities. *Appl Environ Microbiol* **70**: 6147–6156.

Cordes EE, Cunha MR, Galéron J, Mora C, Olu-Le Roy K, Sibuet M *et al.* (2010). The influence of geological, geochemical, and biogenic habitat heterogeneity on seep biodiversity. *Mar Ecol* **31**: 51–65.

Danovaro R, Company JB, Corinaldesi C, D'Onghia G, Galil B, Gambi C *et al.* (2010). Deep-sea biodiversity in the Mediterranean Sea: the known, the unknown, and the unknowable. *PLoS One* **5**: e11832.

Danovaro R, Gambi C, Dell'Anno A, Corinaldesi C, Fraschetti S, Vanreusel A *et al.* (2008). Exponential decline of deep-sea ecosystem functioning linked to benthic biodiversity loss. *Curr Biol* **18**: 1–8.

de Beer D, Sauter E, Niemann H, Kaul N, Foucher J-P, Witte U *et al.* (2006). In situ fluxes and zonation of microbial activity in surface sediments of the Håkon Mosby Mud Volcano. *Limnol Oceanogr* **51**: 1315–1331.

Dufrêne M, Legendre P. (1997). Species assemblages and indicator species: the need to a flexible asymmetrical approach. *Ecol Monogr* **67**: 345–366.

Felden J, Lichtschlag A, Wenzhöfer F, de Beer D, Feseker T, Pop Ristova P *et al.* (2013). Limitations of microbial hydrocarbon degradation at the Amon mud volcano (Nile deep-sea fan). *Biogeosciences* **10**: 3269–3283.

Felden J, Wenzhöfer F, Feseker T, Boetius A. (2010). Transport and consumption of oxygen and methane in different habitats of the Håkon Mosby Mud Volcano (HMMV). *Limnol Oceanogr* **55**: 2366–2380.

Frontier S. (1985). Diversity and structure in aquatic ecosystems. *Oceanogr Mar Biol* **23**: 253–312.

Fuhrman JA, Steele JA, Hewson I, Schwalbach MS, Brown MV, Green JL *et al.* (2008). A latitudinal diversity gradient in planktonic marine bacteria. *Proc Natl Acad Sci USA* **105**: 7774–7778.

Glud RN, Stahl H, Berg P, Wenzhöfer F, Oguri K, Kitazato H. (2009). In situ microscale variation in distribution and consumption of O2: A case study from a deep ocean margin sediment (Sagami Bay, Japan). *Limnol Oceanogr* **54**: 1–12.

Goffredi SK, Orphan VJ. (2010). Bacterial community shifts in taxa and diversity in response to localized

organic loading in the deep sea. *Environ Microbiol* **12**: 344–363.

Green J, Bohannan B. (2006). Spatial scaling of microbial biodiversity. *Trends Ecol Evol* **21**: 501–507.

Grünke S, Felden J, Lichtschlag A, Girnth A, de Beer D, Wenzhöfer F *et al.* (2011). Niche differentiation among mat-forming, sulfide-oxidizing bacteria at cold seeps of the Nile Deep Sea Fan (Eastern Mediterranean Sea). *Geobiology* **9**: 330–348.

Hanson CA, Fuhrman JA, Horner-Devine MC, Martiny JBH. (2012). Beyond biogeographic patterns: processes shaping the microbial landscape. *Nat Rev Microbiol* **10**: 497–506.

He Y, Zhou BJ, Deng GH, Jiang XT, Zhang H, Zhou HW. (2013). Comparison of microbial diversity determined with the same variable tag sequence extracted from two different PCR amplicons. *BMC Microbiol* **13**: 1–8.

Heijs SK, Laverman AM, Forney LJ, Hardoim PR, van Elsas JD. (2008). Comparison of deep-sea sediment microbial communities in the Eastern Mediterranean. *FEMS Microbiol Ecol* **64**: 362–377.

Huber JA, Mark Welch DB, Morrison HG, Huse SM, Neal PR, Butterfield DA *et al.* (2007). Microbial population structures in the deep marine biosphere. *Science* **318**: 97–100.

Inagaki F, Nunoura T, Nakagawa S, Teske A, Lever M, Lauer A *et al.* (2006). Biogeographical distribution and diversity of microbes in methane hydrate-bearing deep marine sediments on the Pacific Ocean Margin. *Proc Natl Acad Sci USA* **103**: 2815–2820.

Jacob M, Soltwedel T, Boetius A, Ramette A. (2013). Biogeography of Deep-sea benthic bacteria at regional scale (LTER HAUSGARTEN, Fram Strait, Arctic). *PLoS One* **8**: e72779.

Jørgensen BB, Boetius A. (2007). Feast and famine — microbial life in the deep-sea bed. *Nature* **5**: 770–781.

Kallmeyer J, Ferdelman TG, Weber A, Fossing H, Jørgensen BB. (2004). A cold chromium distillation procedure for radiolabeled sulfide applied to sulfate reduction measurements. *Limnol Oceanogr Methods* **2**: 171–180.

Knittel K, Boetius A. (2009). Anaerobic oxidation of methane: progress with an unknown process. *Annu Rev Microbiol* **63**: 311–334.

Knittel K, Boetius A, Lemke A, Eilers H, Lochte K, Pfannkuche O *et al.* (2003). Activity, distribution, and diversity of sulfate reducers and other Bacteria in sediments above gas hydrate (Cascadia Margin, Oregon). *Geomicrobiol J* **20**: 269–294.

Kormas KA, Smith DC, Edgcomb V, Teske A. (2003). Molecular analysis of deep subsurface microbial communities in Nankai Trough sediments (ODP Leg 190, Site 1176). *FEMS Microbiol Ecol* **45**: 115–125.

Lawton JH. (1999). Are there general laws in ecology? *Oikos* **84**: 177–192.

Levin LA. (2005). Ecology of cold seep sediment: interactions of fauna with flow, chemistry and microbes. *Oceanogr Mar Biol Annu Rev* **43**: 1–46.

Levin LA, Mendoza GF, Gonzalez JP, Thurber AR, Cordes EE. (2010). Diversity of bathyal macrofauna on the northeastern Pacific margin: the influence of methane seeps and oxygen minimum zones. *Mar Ecol* **31**: 94–110.

Levin LA, Sibuet M. (2012). Understanding continental margin biodiversity: a new imperative. *Ann Rev Mar Sci* **4**: 79–112.

Levin LL, Ziebis W, Mendoza GF, Growney VA, Tryon MD, Brown KB *et al.* (2003). Spatial heterogeneity of macrofauna at northern California methane seeps: influence of sulfide concentration and fluid flow. *Mar Ecol Prog Ser* **265**: 123–139.

Martiny JBH, Bohannan BJM, Brown J, Colwell R, Fuhrman J, Green J *et al.* (2006). Microbial biogeography: putting microorganisms on the map. *Nat Rev Microbiol* **4**: 102–112.

Martiny JBH, Eisen JA, Penn K, Allison SD, Claire Horner-Devine M. (2011). Drivers of bacterial beta-diversity depend on spatial scale. *Proc Natl Acad Sci USA* **108**: 1–5.

Menot L, Galeron J, Olu K, Caprais J-C, Crassous P, Khripounoff A *et al.* (2010). Spatial heterogeneity of macrofaunal communities in and near a giant pockmark area in the deep Gulf of Guinea. *Mar Ecol* **31**: 78–93.

Meyer S, Wegener G, Lloyd K, Teske A, Boetius A, Ramette A. (2013). Microbial habitat connectivity across spatial scales and hydrothermal temperature gradients at Guaymas Basin. *Front Microbiol* **4**: 1–11.

Oksanen J, Blanchet FG, Roeland K, Legendre P, Minchin PR, O'Hara RB *et al.* (2011). vegan: Community Ecology Package. R package version 2.0-2. http://CRAN.R-project.org/package=vegan.

Olu K, Caprais JC, Galéron J, Causse R, von Cosel R, Budzinski H *et al.* (2009). Influence of seep emission on the non-symbiont-bearing fauna and vagrant species at an active giant pockmark in the Gulf of Guinea (Congo–Angola margin). *Deep-Sea Res Pt II* **56**: 2380–2393.

Omoregie EO, Mastalerz V, de Lange G, Straub KL, Kappler A, Røy H *et al.* (2008). Biogeochemistry and community composition of iron- and sulfur-precipitating microbial mats at the Chefren Mud Volcano (Nile Deep Sea Fan, Eastern Mediterranean). *Appl Environ Microbiol* **74**: 3198–3215.

Omoregie EO, Niemann H, Mastalerz V, de Lange G, Stadnitskaia A, Mascle J *et al.* (2009). Microbial methane oxidation and sulfate reduction at cold seeps of the deep Eastern Mediterranean Sea. *Mar Geol* **261**: 114–127.

Orcutt BN, Sylvan JB, Knab NJ, Edwards KJ. (2011). Microbial ecology of the dark ocean above, at, and below the Seafloor. *Microbiol Mol Biol Rev* **75**: 361–422.

Orphan VJ, Hinrichs K, Ussler W III, Paull CK, Taylor LT, Sylva SP *et al.* (2001). comparative analysis of methane-oxidizing archaea and sulfate-reducing bacteria in anoxic marine sediments. *Appl Environ Microbiol* **67**: 1922–1934.

Pachiadaki MG, Lykousis V, Stefanou EG, Kormas KA. (2010). Prokaryotic community structure and diversity in the sediments of an active submarine mud volcano (Kazan mud volcano, East Mediterranean Sea). *FEMS Microbiol Ecol* **72**: 429–444.

Papke R, Ramsing NB, Bateson MM, Ward DM. (2003). Geographical isolation in hot spring cyanobacteria. *Environ Microbiol* **5**: 650–659.

Polymenakou PN, Bertilsson S, Tselepides A, Stephanou EG. (2005). Bacterial community composition in different sediments from the Eastern Mediterranean Sea: a comparison of four 16 S ribosomal DNA clone libraries. *Microb Ecol* **50**: 447–462.

Pommier T, Canbäck B, Riemann L, Boström KH, Simu K, Lundberg P *et al.* (2007). Global patterns of diversity

and community structure in marine bacterioplankton. *Mol Ecol* **16**: 867–880.

Pop Ristova P, Wenzhöfer F, Ramette A, Zabel M, Fischer D, Kasten S *et al.* (2012). Bacterial diversity and biogeochemistry of different chemosynthetic habitats of the REGAB cold seep (West African margin, 3160 m water depth). *Biogeosciences* **9**: 5031–5048.

Pop Ristova P, Wenzhöfer F, Ramette A, Fleden J, Boetius A. (2014). Biogeochemical investigation of cold seep sediments in the Eastern Mediterranean Sea. doi:10.1594/PANGAEA.830241. http://wiki.pangaea.de/wiki/Citation.

Pradillon F, Schmidt A, Peplies J, Dubilier N. (2007). Species identification of marine invertebrate early stages by whole-larvae in situ hybridisation of 18S ribosomal RNA. *Mar Ecol Prog Ser* **333**: 103–116.

Pradillon F, Zbinden M, Mullineaux LS, Gaill F. (2005). Colonisation of newly-opened habitat by a pioneer species, Alvinella pompejana (Polychaeta: Alvinellidae), at East Pacific Rise vent sites. *Mar Ecol Prog Ser* **302**: 147–157.

Quaiser A, Zivanovic Y, Moreira D, López-García P. (2011). Comparative metagenomics of bathypelagic plankton and bottom sediment from the Sea of Marmara. *ISME J* **5**: 285–304.

Ramette A. (2007). Multivariate analyses in microbial ecology. *FEMS Microbiol Ecol* **62**: 142–160.

Ramette A. (2009). Quantitative community fingerprinting methods for estimating the abundance of operational taxonomic units in natural microbial communities. *Appl Environ Microbiol* **75**: 2495–2505.

Ramette A, Tiedje JM. (2007). Multiscale responses of microbial life to spatial distance and environmental heterogeneity in a patchy ecosystem. *Proc Natl Acad Sci USA* **104**: 2761–2766.

Ramirez-Llodra E, Tyler Pa, Baker MC, Bergstad OA, Clark MR, Escobar E *et al.* (2011). Man and the last great wilderness: human impact on the deep sea. *PLoS One* **6**: e22588.

Ritt B, Pierre C, Gauthier O, Wenzhöfer F, Boetius A, Sarrazin J. (2011). Diversity and distribution of cold-seep fauna associated with different geological and environmental settings at mud volcanoes and pockmarks of the Nile Deep-Sea Fan. *Mar Biol* **158**: 1187–1210.

Roberts DW. (2013). labdsv: Ordination and Multivariate Analysis for Ecology. R package version 1.6-1. http://CRAN.R-project.org/package=labdsv.

Rosenzweig ML. (1995). *Species Diversity in Space and Time*. Cambridge University Press: Cambridge, UK.

Ruff SE, Arnds J, Knittel K, Amann R, Wegener G, Ramette A *et al.* (2013). Microbial communities of deep-sea methane seeps at Hikurangi continental margin (New Zealand). *PLoS One* **8**: e72627.

Sahling H, Rickert D, Lee RW, Linke P, Suess E. (2002). Macrofaunal community structure and sulfide flux at gas hydrate deposits from the Cascadia convergent margin, NE Pacific. *Mar Ecol Prog Ser* **231**: 121–138.

Schauer R, Bienhold C, Ramette A, Harder J. (2010). Bacterial diversity and biogeography in deep-sea surface sediments of the South Atlantic Ocean. *ISME J* **4**: 159–170.

Schloss PD, Westcott SL, Ryabin T, Hall JR, Hartmann M, Hollister EB *et al.* (2009). Introducing mothur: open-source, platform-independent, community-supported software for describing and comparing microbial communities. *Appl Environ Microbiol* **75**: 7537–7541.

Seeberg-Elverfeldt J, Schlüter M, Feseker T, Koelling M. (2005). Rhizon sampling of porewaters near the sediment-water interface of aquatic systems. *Limnol Oceanogr Methods* **3**: 361–371.

Sibuet M, Olu K. (1998). Biogeography, biodiversity and fluid dependence of deep-sea cold-seep communities at active and passive margins. *Deep-Sea Res Pt II* **45**: 517–567.

Treude T, Smith CR, Wenzhöfer F, Carney E, Bernardino AF, Hannides AK *et al.* (2009). Biogeochemistry of a deep-sea whale fall: sulfate reduction, sulfide efflux and methanogenesis. *Mar Ecol Prog Ser* **382**: 1–21.

Tyler PA, Young CM. (1999). Reproduction and dispersal at vents and cold seeps. *J Mar Biol Assoc UK* **79**: 193–208.

van Dover C, Smith C, Ardron J, Arnaud S, Beaudoin Y. (2011). Environmental management of deep-sea chemosynthetic ecosystems: justification of and considerations for a spatially-based approach. ISA Technical Study No. 9. International Seabed Authority, Kingston, Jamaica, 2011, 90pp. http://www.isa.org.jm/files/documents/EN/Pubs/TS9/index.html#/.

van Gaever S, Galéron J, Sibuet M, Vanreusel A. (2009). Deep-sea habitat heterogeneity influence on meiofaunal communities in the Gulf of Guinea. *Deep-Sea Res Pt II* **56**: 2259–2269.

Whitaker RJ, Grogan DW, Taylor JW. (2003). Geographic barriers isolate endemic populations of hyperthermophilic archaea. *Science* **301**: 976–978.

Zinger L, Amaral-Zettler LA, Fuhrman JA, Horner-Devine MC, Huse SM, Welch DBM *et al.* (2011). Global patterns of bacterial beta-diversity in seafloor and seawater ecosystems. *PLoS One* **6**: e24570.

Zinger L, Boetius A, Ramette A. (2014). Bacterial taxa-area and distance-decay relationships in marine environments. *Mol Ecol* **23**: 954–964.

Supplementary Information accompanies this paper on The ISME Journal website (http://www.nature.com/ismej)